Topological quantum phases through Majorana wires stablized by many-body localization

Matthew Radzihovsky
Department of Physics, Stanford University, Stanford, CA 94305
(Dated: June 13, 2020)

Submitted as coursework for PH470, Stanford University, Spring 2020

Quantum computing has been vigorously pursued because of its promise of a number of revolutionary applications ranging from cryptography (e.g., Shor's exponential speedup of prime factorization) to solutions of many challenging problems of quantum chemistry and material science. Popular platform candidates include photon time-bin encoded qubits, superconducting qubits, ion trap qubits, among others. However, the emergence of topological qubits theoretically provides a foundation for more robust qubits that store information non-locally and are therefore robust to deleterious effects of local noise. In this paper, we investigate the theory behind Majorana fermions, as appearing at the ends of gated wires of spinless p-wave superconductors, and discuss their utilization for topological quantum computing. We also explore the possibility of expanding the range of stability of the corresponding Majorana phases in the presence of quenched disorder, viewing it through its Jordan-Wigner mapping onto the random transverse field Ising model.

I. INTRODUCTION

A. Motivation

The state of quantum computing has rapidly advanced in recent years due to its allure for solving problems such as integer factorization[1], faster than linear search[2], promise to advance quantum chemistry, and complemented by its relation to fundamental physics from condensed matter to black hole information[3]. In spite of the large advances in quantum computing, the hardware remains at a primitive stage due to challenges of gate errors and decoherence[4]. As a result, quantum computers are limited to solving problems involving few qubits and small number of gate operations. Some of the effects of decoherence and gate errors can be mitigated by quantum error correction (QEC). However, known QEC algorithms require large numbers of ancilla qubit overhead not feasible in current systems[5].

As a revolutionary alternative to overcome the decoherence challenge, Kitaev and Preskill[6] proposed topological quantum computing (TQC) based on topological qubits realized as a set of non-Abelian anyons which encode information non-locally and thus are protected against the detrimental effects of decoherence. In principle, theoretically such anyons and thus TQC can be realized in topological quantum states of matter such as for example weakly-paired 2D p-wave superconductors and the fractional quantum Hall systems. However, a realization is experimentally challenging as it requires ultra clean samples, very low temperatures and states of matter that have not been well established.

Thus a proposal by Oreg et al. and Lutchyn et al.[7,8] reviewed by Alicea[9] to realize TQC through a network of 1D Majorana wires using gated semiconducting wires with strong spin-orbit interaction, proximitized by a conventional s-wave superconductor and an external magnetic field, has attracted lots of attention and has been vigorously explored theoretically and experimentally[8]. In the present paper we focus and review this platform of Majorana wires toward realization of topological quantum computation, highlight the relation to the transverse field Ising model (TFIM) and the Kitaev chain, and analyze the properties of this 1D p-wave superconductor, finding its spectrum and quasi-particles. We review how such wire exhibits gapless Majorana modes localized at its ends and describe their utility for a realization of a topological quantum qubit II[7–10]. Furthermore, we explore using the ideas of many body localization to protect quantum states and information in expanding the applications of quantum computing as explored by Huse et al., Bauer et al., and Kjall et al. III[11–13].

B. Background

Majorana fermions is a particle theoretically proposed by Ettore Majorana in 1937 that is unique in that it is its own antiparticle[14]. A conventional charged particle e.g., an electron is described by a creation and annihilation operator, denoted $c^\dagger_{i,\sigma}$ creates an electron with spin σ at position i, and its Hermitian conjugate $c_{i,\sigma}$ creates a hole at position i. Curiously enough, a Majorana fermion, typically denoted by operator γ, is its own antiparticle, mathematically written as $\gamma^\dagger = \gamma$[9]. However, these Majoranas exist in pairs and can be combined to create a regular fermion by combining Majoranas γ_1 and γ_2 as $f = \frac{1}{2}(\gamma_1 + i\gamma_2)$. Thus, they can be thought of as a "fractionalized zero-mode", namely half of a regular fermion. Thus, a conventional charged (Dirac) fermion constructed with two Majoranas obeys fermionic anti-commutation relation, such that $\{f, f^\dagger\} = 1$ with $\{\gamma_a, \gamma_b\} = 2\delta_{a,b}$. Alternatively, we can write $\gamma_1 = f + f^\dagger$ and $\gamma_2 = \frac{1}{i}(f - f^\dagger)$. The key idea is that if fermion f can be made up of two far separated Majoranas, then this Dirac fermion f can encode non-local information.

This idea is the basis of using Majorana fermions as topological qubits for quantum computing. This ground state degeneracy can encode a "qubit" with the occupation number $\in \{0, 1\}$ representing a qubit. These qubits then can be "braided" (discussed in more detail in section II C 3) together through adiabatic exchange. With information encoded non-locally, errors associated with exchanging Majoranas coming from the environment are significantly less probable than local errors that are currently degrading the efficacy of locally encoded qubits.

II. SIMPLE MODEL

In this section, we start with the familiar transverse-field Ising model (TFIM), and use Jordan-Wigner (JW) transformation to relate it to the seminal Kitaev Majorana chain of spinless p-wave superconductor. We then use the latter to solve the TFIM, to explore its topological properties, and to understand how this model can be used for quantum computing.

A. TFIM to Kitaev chain

A 1D, length L TFIM model is described by the Hamiltonian

$$H = -J \sum_{i=1}^{L} \sigma_i^x \sigma_{i+1}^x - h \sum_{i=1}^{L} \sigma_i^z \tag{1}$$

The Jordan-Wigner transformation (introduced by Jordan and Wigner in 1928) relates spins $\sigma^x, \sigma^y, \sigma^z$ to fermionic creation and annihilation operators $c, c^\dagger$. The components of the spin-1/2 operators are given by $S_{x,y,z} = \frac{1}{2}\sigma^{x,y,z}$, and the corresponding spin raising and lowering operators S_j^+ and S_j^- are

$$S_j^+ = S_j^x + iS_j^y \tag{2}$$
$$S_j^- = S_j^x - iS_j^y \tag{3}$$

with standard spin commutation relation $[S_i^+, S_j^-] = 2S_i^z \delta_{i,j}$. The Jordan-Wigner transformation relates these operators to the fermionic operators c_j, where $c_j^\dagger c_j = n_j$, the occupation number ($n_j \in \{0, 1\}$) mapped from $S^z = \{-\frac{1}{2}, \frac{1}{2}\}$.

$$S_j^+ = c_j^\dagger e^{i\pi \sum_{k<j} c_k^\dagger c_k} \tag{4}$$
$$S_j^- = e^{-i\pi \sum_{k<j} c_k^\dagger c_k} c_j \tag{5}$$
$$S_j^z = c_j^\dagger c_j - \frac{1}{2} \tag{6}$$

These fermionic operators obey fermionic anticommutation relations such that $\{c_i, c_j^\dagger\} = \delta_{ij}$, $\{c_i, c_j\} = \{c_i^\dagger, c_j^\dagger\} = 0$. The exponential operator, often called the Jordan-Wigner "string" introduces an extra minus sign and thereby converts the spin commutation relation on separate sites $[S_j^+, S_i^-] = \delta_{ij} 2S_j^z$ to fermion anticommutation relations $\{c_i, c_j^\dagger\} = \delta_{ij}$ as we demonstrate in detail in the appendix.

Applying the Jordan-Wigner transformation to TFIM, the Hamiltonian becomes:

$$H = -\frac{J}{4} \sum_{i=1}^{L} (c_i^\dagger - c_i)(c_{i+1}^\dagger + c_{i+1}) - \frac{h}{2} \sum_{i=1}^{L} c_j^\dagger c_j - c_j c_j^\dagger \tag{7}$$

This is the celebrated Kitaev Hamiltonian studied extensively since its introduction by Kitaev[6]:

$$H = -\mu \sum_i c_i^\dagger c_i - \frac{1}{2} \sum_i (t c_i^\dagger c_{i+1} + \Delta c_i c_{i+1} + h.c.) \tag{8}$$

where $\mu = h$, $\Delta = t = J$ when JW transformed from the TFIM. We can classify each term, namely μ is the chemical potential, $t \geq 0$ is the hopping amplitude, and Δ is a complex p-wave superconducting pairing amplitude. This mapping provides an exact solution of the TFIM in terms of the quadratic Kitaev Hamiltonian that is easily diagonalized by going to momentum basis (Fourier transforming) and then doing Bogoluibov transformation.

B. Kitaev chain with periodic boundary conditions

We first consider a 1D chain with *periodic* boundary conditions (i.e., closed chain with no ends). This translationally invariant system allows us to apply a Fourier transform by switching to the momentum basis using $c_j = \frac{1}{\sqrt{N}} \sum_k e^{ikj} c_k$ and $c_j^\dagger = \frac{1}{\sqrt{N}} \sum_k e^{-ikj} c_k^\dagger$ (with k limited to the 1st Brillouin zone, $-\pi < k < \pi$), we find:

$$\begin{aligned} H = &-\mu \sum_k c_k^\dagger c_k \\ &- \sum_k (t \cos(k) c_k^\dagger c_k - \Delta (c_k^\dagger c_{-k}^\dagger e^{ik} + c_{-k} c_k e^{-ik}) \end{aligned} \tag{9}$$

Standard analysis allows us to rewrite the Kitaev chain

Hamiltonian in a more convenient form:

$$H = \frac{1}{2}\sum_k(-t\cos(k)-\mu)(c_k^\dagger c_k + c_{-k}^\dagger c_{-k}) + \frac{1}{2}\sum_k(i\Delta\sin(k)(c_k^\dagger c_{-k}^\dagger + c_{-k}c_k) \tag{10}$$

This can more simply be written in matrix form in terms of single particle spectrum $\epsilon_k = -t\cos k - \mu$ and $\tilde{\Delta}_k = -i\Delta\sin k$. Defining $\vec{\psi}_k = (c_k, c_{-k}^\dagger)$, the Hamiltonian can be written:

$$H = \frac{1}{2}\sum_k \psi_k^\dagger \cdot \mathcal{H}_k \cdot \psi_k + \sum_k \epsilon_k \tag{11}$$

where

$$\mathcal{H} = \begin{pmatrix} \epsilon_k & \tilde{\Delta}_k^* \\ \tilde{\Delta}_k & -\epsilon_k \end{pmatrix} \tag{12}$$

which can be diagonalized by unitary transformation :

$$U_k = \begin{pmatrix} u_k & v_k \\ -v_k^* & u_k^* \end{pmatrix} \tag{13}$$

Thus, inserting an identity $1 = U^\dagger U$ and choosing U to diagonalize $\mathcal{H}$, we find,

$$H = \frac{1}{2}\sum_k \psi_k^\dagger U_k^\dagger U_k \mathcal{H}_k U_k^\dagger U_k \psi_k \tag{14}$$

$$= \frac{1}{2}\sum_k \tilde{\psi_k}^\dagger \tilde{\mathcal{H}}_k \tilde{\psi}_k \tag{15}$$

where $\tilde{\psi_k} = U_k\psi_k = (a_k, a_{-k}^\dagger)$. Thus,

$$\tilde{\psi_k} = \begin{pmatrix} a_k \\ a_{-k}^\dagger \end{pmatrix} = \begin{pmatrix} u_k & v_k \\ -v_k^* & u_k^* \end{pmatrix}\begin{pmatrix} c_k \\ c_{-k}^\dagger \end{pmatrix} \tag{16}$$

Therefore, $a_k = u_k c_k + v_k c_{-k}^\dagger$ where from diagonalization, eigenvalues and eigenvectors are found:

$$E_\pm(k) = \pm\sqrt{\epsilon_k^2 + |\tilde{\Delta}_k|^2} = \pm E_k \tag{17}$$

and

$$u_k = \frac{\tilde{\Delta}_k}{|\tilde{\Delta}_k|}\frac{\sqrt{E_k+\epsilon_k}}{\sqrt{2E_k}} \tag{18}$$

$$v_k = \left(\frac{E_k - \epsilon_k}{\tilde{\Delta}_k}\right)u_k \tag{19}$$

Thus, the Hamiltonian becomes:

$$H = \frac{1}{2}\sum_k E_k a_k^\dagger a_k - E_k a_{-k} a_{-k}^\dagger + \sum_k \epsilon_k \tag{20}$$

$$= \sum_k E_k a_k^\dagger a_k - \frac{1}{2}(E_k - \epsilon_k) \tag{21}$$

$$= \sum_k E_k a_k^\dagger a_k + E_{gs}(\Delta) \tag{22}$$

where

$$E_k = \sqrt{\epsilon_k^2 + |\tilde{\Delta}_k|^2} \tag{23}$$

is the fully gapped excitation spectrum of the closed Kitaev chain (p-wave superconductor) and

$$E_{gs}(\Delta) = -\sum_k \frac{1}{2}(E_k - \epsilon_k) \tag{24}$$

is the ground state of the Bardeen-Cooper-Schrieffer (BCS) p-wave superconducting state, which is negative relative to the normal state and thus energetically preferred at zero temperature.

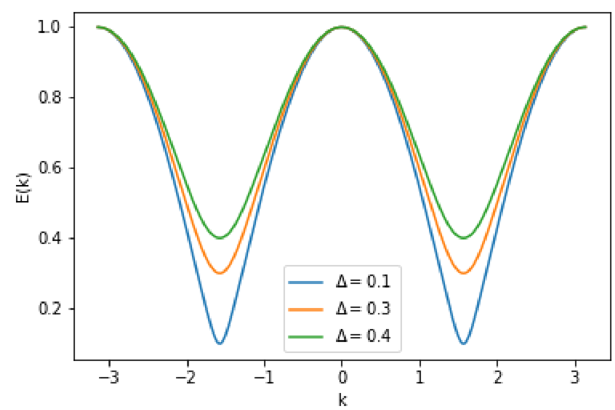

Figure 1: Fully gapped spectrum E_k of the 1D p-wave superconductor (Kitaev chain) with periodic boundary conditions for $\mu = 0$, $t = 1$ and for $\Delta = 0.1, 0.3, 0.4$. As is clear from Eq. 17, the plots approximately resemble $|\epsilon_k|$ but with the added superconducting gap Δ at the Fermi points at $k_F = \pm\frac{\pi}{2}$ due to superconducting pairing.

C. Kitaev Chain with open boundaries

In previous section we analyzed a boundaries-free Kitaev chain and found that its spectrum Eq. 17 is fully gapped. We now focus on the chain with open boundary conditions (two ends), a case that is relevant to the TQC application as it realizes Majorana zero modes at the ends of the wire of a topological phase.

1. *Phases*

Using the rewritten TFIM Hamiltonian as a Kitaev chain, from Eq. 17 it is apparent that by tuning μ, a gap closes as μ approaches $\pm t$ where $\epsilon_\pi = -t\cos(\pi) - t = 0$ and $\Delta_\pi = \Delta\sin(\pi) = 0$. In Figure 3, we plot the kinetic energy of the 1D Kitaev chain versus k. It is clear that

Figure 2: Kitaev chain of fermionic particles from Eq. 30. Pairing of Majoranas at the same lattice site denoted by μ contrasted with pairing of Majoranas at adjacent sites illustrating $\gamma_{A,1}$ and $\gamma_{B,L}$ unpaired as "fractionalized zero-modes" with two-fold degeneracy (based on Ref. 9).

for $\mu = \pm t$ the Kitaev chain has gapless bulk excitations, namely when μ is exactly tuned to the top or bottom of the band.

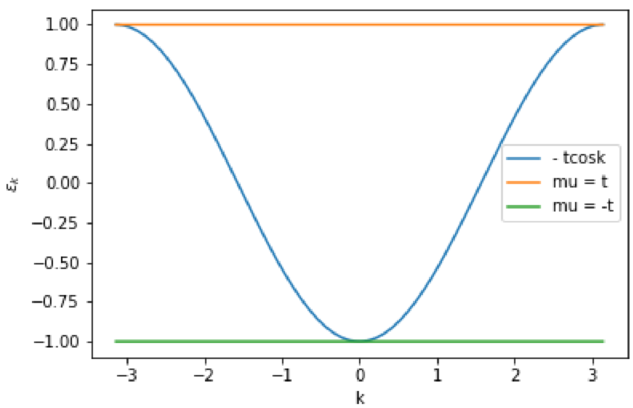

Figure 3: A spectrum ϵ_k of a non-superconducting fermionic chain, illustrating the range of chemical potentials μ. For $\mu < -t$, the state is a vacuum of electrons and is thus a trivial insulator. Same is true for the full band for $\mu > t$. However, as discussed in the text, for $-t < \mu < t$ the corresponding p-wave paired state is a topological superconductor (based on Ref. 9).

In Figure 4, we display how the relationship between the chemical potential μ and the hopping term coefficient t creates either a topological phase (weak pairing for $-t < \mu < t$) or a non-topological/trivial phase (strong pairing for $|\mu| > t$). Experimentally, this suggests by tuning the chemical potential of the Kitaev chain, we can create Kitaev chains with gapless Majorana modes appearing at its ends where chemical potential $|\mu|$ crosses t, with vaccuum outside the wire interpreted as the trivial insulating state with $|\mu| > t$.

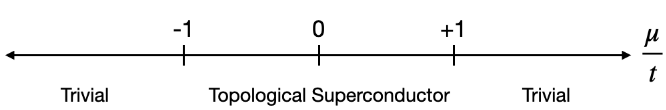

Figure 4: Tuning of $\frac{\mu}{t}$ for different phases. Trivial represents a non-topological insulator phase.

2. Majorana Representation

Introducing real and imaginary parts of the conventional fermion $c_x = \frac{1}{2}(\gamma_{B,x} + i\gamma_{A,x})$, we can now express the Hamiltonian for the p-wave superconductor, Eq. 8, in terms of the Majorana fermions $\gamma_{B,x}$ and $\gamma_{A,x}$. Taking $\{\gamma_A, \gamma_B\} = 2\delta_{A,B}$ guarantees that c_x satisfy the requisite anticommutation relation $\{c_x, c^\dagger_{x'}\} = \delta_{x,x'}$. To rewrite the Hamiltonian, we recognize

$$c^\dagger_x c_x = \frac{1}{4}\left(\gamma_{B,x} - i\gamma_{A,x}\right)\left(\gamma_{B,x} + i\gamma_{A,x}\right) \tag{25}$$

$$= \frac{1}{2}\left(1 + i\gamma_{B,x}\gamma_{A,x}\right) \tag{26}$$

and

$$(c^\dagger_x + c_x)(c_{x+1} - c^\dagger_{x+1}) = i\gamma_{B,x}\gamma_{A,x+1} \tag{27}$$

Finally, for convenience and because we are interested in universal properties, let us set $\Delta = t$ (corresponding to JW mapping from the TFIM to Hamiltonian in Eq. 7), and take open boundary conditions, obtaining .

$$H = -\mu\sum_x c^\dagger_x c_x - \frac{1}{2}\sum_x (tc^\dagger_x c_{x+1} + \Delta c_x c_{x+1} + h.c.) \tag{28}$$

$$= \sum_x -\mu c^\dagger_x c_x - \frac{t}{2}(c^\dagger_x + c_x)(c_{x+1} - c^\dagger_{x+1}) \tag{29}$$

$$= \frac{-i}{2}\sum_x \left(\mu\gamma_{B,x}\gamma_{A,x} + t\gamma_{B,x}\gamma_{A,x+1}\right) \tag{30}$$

where we drop an unimportant constant.

This Hamiltonian clearly reveals two pairing terms, namely the μ term for same site Majorana pairing $(\gamma_{B,x}\gamma_{A,x})$ and the t term across neighboring sites Majorana pairing $(\gamma_{B,x}\gamma_{A,x+1})$. Thus, if $t = 0$ and $\mu < 0$, we have a trivial insulator state with no entanglement between Majoranas on different sites. In contrast, for $\mu = 0$ and $t > 0$ the Majorana fermions are paired across neighboring sites as illustrated in Fig. 2. As we discussed previously (see Figs. 3 and 4) this latter case corresponds to the topological superconductor. To see this, note that for this case of $\mu = 0$ the two end Majorana modes $\gamma_{B,L}$ and $\gamma_{A,1}$ do not appear in the Hamiltonian in Eq. 30. Thus, we can form a highly non-local Dirac fermion from these Majoranas, given by

$$d = \frac{1}{2}\left(\gamma_{B,L} + i\gamma_{A,1}\right) \tag{31}$$

This d is a Dirac fermion whose state can either be filled or empty with no energy cost. Thus, this non-local fermion acts as a non-local qubit due to the two-fold degeneracy as its real and imaginary Hermitian components consist of Majorana fermions $\gamma_{A,1}$ and $\gamma_{B,L}$ localized at far separated ends of the superconducting chain at $i = 1$

and $i = L$ respectively. The two corresponding states in terms of the BCS round state $|\mathrm{BCS\ GS}\rangle$ are given by:

$$|0\rangle = |\mathrm{BCS\ GS}\rangle\,, \quad d^\dagger\,|0\rangle = |1\rangle \tag{32}$$

where each state carries opposite fermion parity which allows the encoding of local information non-locally. Further note, that for a more general case where $\mu \neq 0$ and $\Delta \neq t$, Alicea[9] shows that these zero-modes decay exponentially into the bulk such that there is an exponentially decaying energy difference between the ground states, namely $E \sim e^{(-L\log(J/h))}$. Thus, in the thermodynamic limit of long wires, the qubit states are degenerate.

3. Braiding

With the understanding of the setup for the creation of Majorana fermions, we introduce a swapping operator that allows the entanglement of Majorana qubits and the possibility of performing more complex computation. In the 1D Kitaev chain model, where the ends of the chain are the Ising non-Abelian anyons, these end Majoranas can be exchanged revealing non-Abelian statistics. As shown in the prior section, each fermion is made up two Majoranas, namely the first sites and last sites denoted pieces denoted $d = \frac{1}{2}(\gamma_{B,L} + i\gamma_{A,1})$.

A swapping operator U_{ij} encodes these non-Abelian statistics $\psi_i \rightarrow U_{ij}\psi_j$ where U_{ij} is a unitary transformation. Given two chains $d_1 = \frac{1}{2}(\gamma_1 + i\gamma_2)$ and $d_2 = \frac{1}{2}(\gamma_3 + i\gamma_4)$, "fermionic halves" or Majoranas from each fermion can be braided. For example, if we wish to swap γ_1 and γ_3, we can use $U_{13} = e^{\pm\frac{\pi}{4}\gamma_1\gamma_3} = \frac{1}{\sqrt{2}}(1 + \gamma_1\gamma_3)$. Upon a clockwise rotation, the exchange will send $\gamma_1 \rightarrow -\gamma_3$ and $\gamma_3 \rightarrow \gamma_1$ revealing the non-Abelian statistics and converting the corresponding annihilation operator $\gamma_1 + i\gamma_3$ into a creation operator $\gamma_1 - i\gamma_3$. For many Majorana ends, say 2n, the order of the exchanges effects the final state of the system and is thus U_{ij} is a non-Abelian operator. These exchange operations extend to 2D topological superconductors with Majoranas localized on vortices that can be created with an external magnetic field. Experimentally, this can be done by tuning the chemical potential μ to move around the Majorana end-of-wires and exchange the γ's from separate fermions.

4. P-wave SC

Although as we have seen the Kitaev chain can be directly realized by a spinless p-wave superconductor, to do this directly is quite challenging as p-wave superconductors are difficult to realize. Instead, as proposed by Oreg, et al.[7] and Lutchyn et al.[8], the effective 1D p-wave superconductor (Kitaev chain) can be realized with quite conventional ingredients of a semiconducting wire with strong spin-orbit interaction, proximitized with conventional (abundant e.g. Aluminum) s-wave superconductor, in an applied magnetic field. In more detail and specifically, first, in a 1D wire system in proximity to an s-wave superconductor will create an overlapping parabolic band structure for both spins. These bands can be separated in momentum space by adding Rashba spin-orbit coupling such that the band structure of spin up moves toward positive momentum and vice versa for spin downs. Thus, there is a single point of overlapping band structure for each spin at zero momentum. To break this time-reversal symmetry, apply an external magnetic field, which breaks the bands into lower and higher bands seperated by a Zeeman gap. With the chemical potential tuned between these two bands, this allows for the realization of a topological p-wave superconducter for large enough $\frac{B}{\Delta}$, and a trivial state for $B << \Delta$.

III. LOCALIZATION FOR PROTECTED QUANTUM ORDER

In this section we explore the possibility of using localization protected quantum order and implications for localized phases including topological order that, in theory, could expand the applications or realizations of quantum computing. The eigenstate thermalization hypothesis (ETH) describes thermal behavior of isolated quantum systems. However, this hypothesis breaks down in integrable systems, and localized systems (so-called many-body localized). Originally described by Anderson localization in 1958 with non-interacting particles and then expanded to interacting isolated many-body systems, these localization phases called many-body localized (MBL)[15,11] have "quantum memory" of their initial state as they do not thermalize.

A. Thermalization to Many Body Localization

Classical systems and traditional statistical mechanics rely on the ergodicity hypothesis and averages, namely that all microstates of a system have the same probability of realization and that at long times, averages are taken to understand the dynamics of a system. As explored by Deutsch[16] and Srednicki[17], ETH extends the microcanonical ensemble to eigenstates with thermal observables. Even within isolated quantum systems, the system can be broken up into an effective heat bath, where the remaining subsystem experiences thermalization where at long times, observables "thermalize" described by the microcanonical ensemble. This can be seen by using random matrices to look at level statistics where we see Wigner-Dyson statistics (level spacing probability density goes as $s^\beta e^{-s^2/2}$ for spacing s and $\beta = 1, 2, 4$) and corresponding to level repulsion. Furthermore, this can be seen as the von Neumann entanglement entropy of subsystem A for an eigenstate approaches the thermodynamic entropy at long times. Mathematically, the entanglement entropy for eigenstate $|\alpha\rangle$ is defined by density matrix $\rho_A = tr_B \rho_{AB} = tr_B |\alpha\rangle \langle\alpha|$ as $S_E = -tr \rho_A \log \rho_A$. Thus, for a thermalizing system we find that the entanglement entropy scales with the volume of the system:

$$S_{\mathrm{E}}(A) = -tr\rho_A \log \rho_A = S_{therm}(A) \tag{33}$$

However, this hypothesis can breakdown in the presence of quenched disorder when the system can become many-body localized, an interacting version of Anderson localization. MBL has been shown to survive to non-zero energy density at sufficiently strong disorder, weak interactions, as illustrated in Fig. 5 and 6. To examine this, let us look at a XXZ-spin chain with disorder:

$$H_{XXZ} = J_{x,y} \sum_i^L (\sigma_i^x \sigma_{i+1}^x + \sigma_i^y \sigma_{i+1}^y) + J_z \sum_i^L \sigma_i^z \sigma_{i+1}^z + h_i \sigma_i^z \tag{34}$$

where $J_{x,y}$, J_z are the spin exchange and $h_i \in \{-W, W\}$ is the random fields. Once again, using a Jordan-Wigner transformation, this spin model maps onto a spinless fermionic particles c_i with number density operator $n_i = c_i^\dagger c_i$ as follows:

$$H = t \sum_i (c_i^\dagger c_{i+1} + h.c) - V \sum_i n_i n_{i+1} + \sum_i \epsilon_i n_i \tag{35}$$

where $t = J_{x,y}$ is the hopping amplitude, $V = J_z$ is the fermion interaction, and $\epsilon_i = h_i$ is the random chemical potential.

From this system, we can get a general phase diagram as we vary interactions J_z and disorder W, namely:

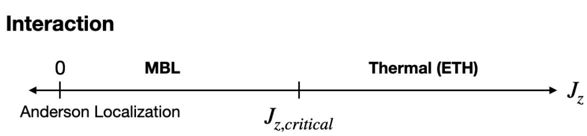

Figure 5: Tuning of J_z for fixed disorder and energy density, illustrating the transition from MBL to ETH (based on Ref. 15)

.

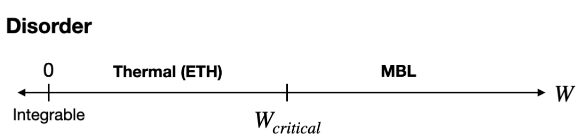

Figure 6: Tuning of W for fixed interaction and energy density, illustrating the transition from ETH to MBL (based on Ref. 15)

.

Contrary to the thermalization phase in the MBL state, the level statistics obey a Poisson distribution and there is no level repulsion. Furthermore, the entanglement entropy scales with the area of the system, as well as starting from initial product states, the entanglement entropy grows logarithmically, and at late time saturates to a proportion of the system size (smaller than the expected thermal equilibrium entanglement entropy). This differs from both the thermalizing phase, but also Anderson localization without interactions[15].

B. Localization Protected Quantum Order

In this section, we explore how localization can be used to protect quantum phases. In these models, we are interested in how localization can provide long range order and spontaneous symmetry breaking, which surprisingly can protect quantum order and quantum phases.

1. *Transverse Field Ising Model with disorder*

The TFIM Hamiltonian without disorder described by

$$H = J \sum_i \sigma_i^{(z)} \sigma_{i+1}^{(z)} + h \sum_i \sigma_i^{(x)} \tag{36}$$

has been studied and shown that at thermodynamic equilibrium there is no discrete spontaneous symmetry breaking at a finite temperature for dimensions $d = 1$, and no continuous spontaneous symmetry breaking at a finite temperature for dimensions $d = 1, 2$. In 1D, for $h = 0$, there are two degenerate ground states, namely $|\uparrow\uparrow ... \uparrow\rangle$ and $|\downarrow\downarrow ... \downarrow\rangle$. As h increases, domain walls emerge with a cost only paid at the domain wall site. Therefore, for small $\frac{h}{J}$ limit, perturbation theory shows that it is possible to flip every spin to connect the previous degenerate ground states, $|\uparrow\uparrow ... \uparrow\rangle$ and $|\downarrow\downarrow ... \downarrow\rangle$. Thus, at finite h, there is symmetric and antisymmetric ground states, denoted $|\pm\rangle = |\uparrow\uparrow ... \uparrow\rangle \pm |\downarrow\downarrow ... \downarrow\rangle$. As $\frac{h}{J}$ increases, each spin points along the external field with a non-degenerate ground state denoted $|\rightarrow, \rightarrow, ... \rightarrow\rangle$. In this case, there is still no long range order, as well as no net magnetization for the z-direction of interest. This is the PM state.

Thus, there are two apparent phases at finite temperature:

1. Ferromagnet phase, small $\frac{h}{J}$
   Degenerate ground states at temperature $= 0$: $|\pm\rangle = |\uparrow\uparrow ... \uparrow\rangle \pm |\downarrow\downarrow ... \downarrow\rangle$
   At finite temperature, it is apparent that there is no long range order because the domain walls mix and freely move between each spin. The domain walls fluctuate throughout the chain and thus there is no spontaneous symmetry breaking.

2. Paramagnet phase, large $\frac{h}{J}$
   Ground state at temperature $= 0$: $|\rightarrow, \rightarrow, ... \rightarrow\rangle$

At finite temperature, there is no long range order and no net magnetization along z.

In order to create long range order, as shown in the previous section, we add disorder to the model. The disorder TFIM Hamiltonian is:

$$H = \sum_i J_i \sigma_i^{(z)} \sigma_{i+1}^{(z)} + h_i \sigma_i^{(x)} \tag{37}$$

By adding disorder the domain walls are pinned. Therefore, the system can display a spin glass phase that has spontaneous symmetry breaking based on where the domain walls sit within the chain with a frozem pattern of σ_z spins along the chain. Since each domain wall has its own cost due to randomness, then each domain wall state is separated out rather than being degenerate without disorder. Therefore, there is long range order at finite energy density. This can be seen by looking at correlation function order parameter $\langle \sigma_i^{(z)} \sigma_{i+1}^{(z)} \rangle$ for eigenstates $|\tilde{\pm}\rangle$ where Huse et al. show that $\langle \tilde{\pm} | \sigma_{i+1}^{(z)} | \tilde{\pm} \rangle \neq 0$.

Therefore, the phase diagram as a function of $\frac{h}{J}$ includes a dynamical phase transition from a many-body localized spin glass state at small $\frac{h}{J}$ to a paramagnetic state at large $\frac{h}{J}$. In the MBL spin glass state, the ground states are spontaneously chosen as frozen "cat" states such as $|\uparrow, \uparrow, \downarrow, \ldots\rangle + |\downarrow, \downarrow, \uparrow, \ldots\rangle$. In the paramagnetic state, the ground states are random spins in the x-basis, namely $|\rightarrow, \rightarrow, \leftarrow, \ldots\rangle$.

In fact, Kjall et al. simulates a quantum Ising chain for next nearest neighbors with disorder only in the interaction term described by,

$$H = \sum_i J_i \sigma_i^{(z)} \sigma_{i+1}^{(z)} + J_2 \sum_i \sigma_i^{(z)} \sigma_{i+2}^{(z)} + h \sum_i \sigma_i^{(x)} \tag{38}$$

where J_i is randomly drawn from $\{-\delta J, \delta J\}$. this model becomes the TFIM when $J_2 = \delta_J = 0$, namely when there are no next-nearest neighbor interaction and no disorder for J_i. In this variant model, as disorder increases, once again a thermal and MBL spin glass phase arise, but now there is an MBL paramagnetic phases between the two that is characterized by domain walls which are created and removed in pairs.[13]

2. *Topological Phases*

Localization in the disordered TFIM has been extended to the possibility of theoretically protecting topological order[11][12]. Huse et al. explores the topological order of the Kitaev chain that relies on the two Majoranas at each end of the chain not interacting with the bulk. Thus, the addition of any interactions destroys this topological order. However, by adding disorder, it is shown that with interactions and without a gap, topological order of the chain is protected. From the Kitaev Hamiltonian in II C, note that fermionic parity is maintained from terms $c_i^\dagger c_{i+1}^\dagger$ and $c_i c_{i+1}$. Since parity is maintained, adding short range interaction does not effect the edge Majoranas. Finally, the bulk is Dirac and many-body localized due to the disorder, which ensures that the particles or energy does not propagate through the system. Therefore, by adding disorder, the MBL bulk protects this topological order.

Bauer et al. explores further, investigating implications of protected topological order for quantum computing, specifically topological quantum error correcting code. The Toric code model is defined by spins on a 2D lattice with periodic boundary conditions and by Hamiltonian:

$$H = -J \sum_v A_v - J \sum_p B_p \tag{39}$$

where $A_v = \prod_{i \in v} \sigma_i^{(x)}$ is the vertex term where all sites touching the vertex are included and $B_p = \prod_{i \in p} \sigma_i^{(z)}$ is the plaquette terms which includes all terms around the plaquette. This model has excitations which can map onto anyons discussed in II and motivates topological quantum error correction. Including disorder in such a model can localize the system and improve the quantum memory. Furthermore, disorder and localization can even give rise to self-correcting quantum memories.

IV. SUMMARY

In this paper, we investigated the realization of Majorana fermions in spinless p-wave superconductors as proposed by Oreg et al. and Lutchyn et al. Applying JW transformation, we related p-wave superconductor to TFIM and used it to solve this model computing its spectrum and quasiparticles using Fourier analysis and Bogoliubov transformation. We also explore the possibility of expanding the range of stability of the corresponding Majorana phases in the presence of quenched disorder even at finite energy density, utilizing the many-body localized states that are predicted to appear.

[1] Peter W Shor. Polynomial-time algorithms for prime factorization and discrete logarithms on a quantum computer. *SIAM review*, 41(2):303–332, 1999.

[2] Lov K Grover. A fast quantum mechanical algorithm for database search. *arXiv preprint quant-ph/9605043*, 1996.

[3] Benjamin P Lanyon, James D Whitfield, Geoff G Gillett,

Michael E Goggin, Marcelo P Almeida, Ivan Kassal, Jacob D Biamonte, Masoud Mohseni, Ben J Powell, Marco Barbieri, et al. Towards quantum chemistry on a quantum computer. *Nature chemistry*, 2(2):106, 2010.

[4] Thaddeus D Ladd, Fedor Jelezko, Raymond Laflamme, Yasunobu Nakamura, Christopher Monroe, and Jeremy Lloyd O'Brien. Quantum computers. *nature*, 464(7285):45, 2010.

[5] Edward Farhi, Jeffrey Goldstone, Sam Gutmann, and Michael Sipser. Quantum computation by adiabatic evolution. *arXiv preprint quant-ph/0001106*, 2000.

[6] Alexei Kitaev and John Preskill. Topological entanglement entropy. *Physical Review Letters*, 96(11), Mar 2006.

[7] Yuval Oreg, Gil Refael, and Felix von Oppen. Helical liquids and majorana bound states in quantum wires. *Phys. Rev. Lett.*, 105:177002, Oct 2010.

[8] Roman M. Lutchyn, Jay D. Sau, and S. Das Sarma. Majorana fermions and a topological phase transition in semiconductor-superconductor heterostructures. *Phys. Rev. Lett.*, 105:077001, Aug 2010.

[9] Jason Alicea. New directions in the pursuit of majorana fermions in solid state systems. *Reports on Progress in Physics*, 75(7):076501, Jun 2012.

[10] Jason Alicea, Yuval Oreg, Gil Refael, Felix von Oppen, and Matthew P. A. Fisher. Non-abelian statistics and topological quantum information processing in 1d wire networks. *Nature Physics*, 7(5):412–417, Feb 2011.

[11] David A. Huse, Rahul Nandkishore, Vadim Oganesyan, Arijeet Pal, and S. L. Sondhi. Localization-protected quantum order. *Physical Review B*, 88(1), Jul 2013.

[12] Bela Bauer and Chetan Nayak. Area laws in a many-body localized state and its implications for topological order. *Journal of Statistical Mechanics: Theory and Experiment*, 2013(09):P09005, Sep 2013.

[13] Jonas A. Kjäll, Jens H. Bardarson, and Frank Pollmann. Many-body localization in a disordered quantum ising chain. *Physical Review Letters*, 113(10), Sep 2014.

[14] N. Majorana. A symmetric theory of electrons and positrons. *Ettore Majorana Scientific Papers: On occasion of the centenary of his birth*, pages 201–233, 01 2006.

[15] Dmitry A. Abanin, Ehud Altman, Immanuel Bloch, and Maksym Serbyn. Colloquium : Many-body localization, thermalization, and entanglement. *Reviews of Modern Physics*, 91(2), May 2019.

[16] J. M. Deutsch. Quantum statistical mechanics in a closed system. *Phys. Rev. A*, 43:2046–2049, Feb 1991.

[17] Mark Srednicki. Chaos and quantum thermalization. *Physical Review E*, 50(2):888–901, Aug 1994.

Appendix A: Appendix A: Applying the Jordan-Wigner Transformation to TFIM

The details of the Jordan-Wigner transformation taking the TFIM model to the Kitaev chain model is described here. In the one-dimensional spin basis, a length L TFIM model is described by the Hamiltonian

$$H = -J\sum_{i=1}^{L}\sigma_i^x\sigma_{i+1}^x - h\sum_{i=1}^{L}\sigma_i^z \tag{A1}$$

The components of the spin-1/2 operators are given by $S_{x,y,z} = \frac{1}{2}\sigma^{x,y,z}$, and the corresponding spin raising and lowering operators S_j^+ and S_j^- are

$$S_j^+ = S_j^x + iS_j^y \tag{A2}$$

$$S_j^- = S_j^x - iS_j^y \tag{A3}$$

with standard spin commutation relation $[S_i^+, S_j^-] = 2S_i^z\delta_{i,j}$. The Jordan-Wigner transformation relates these operators to the fermionic operators c_j, where $c_j^\dagger c_j = n_j$, the occupation number ($n_j \in \{0,1\}$) mapped from $S^z = \{-\frac{1}{2}, \frac{1}{2}\}$.

$$S_j^+ = c_j^\dagger e^{i\pi\sum_{k<j} c_k^\dagger c_k} \tag{A4}$$

$$S_j^- = e^{-i\pi\sum_{k<j} c_k^\dagger c_k} c_j \tag{A5}$$

$$S_j^z = c_j^\dagger c_j - \frac{1}{2} \tag{A6}$$

These fermionic operators obey fermionic commutation and anticommutation relations such that $\{c_i, c_j^\dagger\} = \delta_{ij}$, $\{c_i, c_j\} = \{c_i^\dagger, c_j^\dagger\} = 0$. The exponential terms, often called the Jordan-Wigner "string" translates the spin commutation on separate sites $[S_j^+, S_i^-] = \delta_{ij}2S_j^z$ to obey fermion anticommutation relations $\{c_i, c_j^\dagger\} = \delta_{ij}$.

To explicitly see this, let us look at $[S_j^+, S_k^-]$ for two cases, $j = k$ and $j < k$. In general, this commutation is described by:

$$\begin{aligned}[S_j^+, S_k^-] &= c_j^\dagger e^{i\pi\sum_{l<j} c_l^\dagger c_l} e^{-i\pi\sum_{m<k} c_m^\dagger c_m} c_k \\ &\quad - e^{-i\pi\sum_{m<k} c_m^\dagger c_m} c_k c_j^\dagger e^{i\pi\sum_{l<j} c_l^\dagger c_l}\end{aligned}$$

Case 1: $j = k$**.** For $j = k$, since the string operators only include c_l for $l < j$ and $l < k$, then we can freely rearrange the terms since $\{c_i, c_j^\dagger\} = \delta_{ij}$.

$$\begin{aligned}[S_j^+, S_j^-] &= c_j^\dagger e^{i\pi\sum_{l<j} c_l^\dagger c_l} e^{-i\pi\sum_{l<j} c_l^\dagger c_l} c_j \\ &\quad - e^{-i\pi\sum_{l<j} c_l^\dagger c_l} c_j c_j^\dagger e^{i\pi\sum_{l<j} c_l^\dagger c_l} \\ &= c_j^\dagger c_j - c_j c_j^\dagger \\ &= n_j - (1 - n_j) \\ &= 2(n_j - \frac{1}{2}) \\ &= 2S_j^z\end{aligned}$$

Case 2: $j < k$**.** For $j < k$, since the string operators only include c_l for $l < j$ and $l < k$, then since $\{c_i, c_j^\dagger\} = \delta_{ij}$, the only term that is interesting when rearranging arises from $[e^{-i\pi c_j^\dagger c_j}, c_j^\dagger]$. From Taylor expanding $e^{-i\pi c_j^\dagger c_j}$ or recognizing $c_j^\dagger c_j = n_j \in \{0,1\}$, we can rewrite $e^{-i\pi c_j^\dagger c_j} = 1 - 2c_j^\dagger c_j$. Therefore, we find:

$$
\begin{aligned}
[e^{-i\pi c_j^\dagger c_j}, c_j^\dagger] &= (1-2c_j^\dagger c_j)c_j^\dagger - c_j^\dagger(1-2c_j^\dagger c_j) \\
&= -2c_j^\dagger c_j c_j^\dagger \\
&= -2c_j^\dagger(1-2c_j^\dagger c_j) \\
&= -2c_j^\dagger e^{-i\pi c_j^\dagger c_j}
\end{aligned}
$$

Thus, the commutation relation simplifies to:

$$
\begin{aligned}
[S_j^+, S_k^-] &= c_j^\dagger e^{i\pi\sum_{l<j} c_l^\dagger c_l} e^{-i\pi\sum_{m<k} c_m^\dagger c_m} c_k \\
&- e^{-i\pi\sum_{m<k} c_m^\dagger c_m} c_k c_j^\dagger e^{i\pi\sum_{l<j} c_l^\dagger c_l} \\
&= c_j^\dagger c_k e^{i\pi\sum_{l<j} c_l^\dagger c_l} e^{-i\pi\sum_{m<k} c_m^\dagger c_m} \\
&- c_k c_j^\dagger e^{-i\pi\sum_{m<k} c_m^\dagger c_m} e^{i\pi\sum_{l<j} c_l^\dagger c_l} \\
&= \{c_j^\dagger, c_k\} e^{i\pi\sum_{l<j} c_l^\dagger c_l} e^{-i\pi\sum_{m<k} c_m^\dagger c_m} \\
&= 0
\end{aligned}
$$

Thus, with the Jordan-Wigner strings, the commutation relations from the spin operators hold. Using $\sigma^x = S^+ + S^-$ and plugging in the above transformations into the TFIM Hamiltonian, the Hamiltonian transforms:

$$
\begin{aligned}
H &= -J\sum_{i=1}^{L} \sigma_i^x \sigma_{i+1}^x - h\sum_{i=1}^{L} \sigma_i^z \\
&= -J\sum_{i=1}^{L} (S_i^+ + S_i^-)(S_{i+1}^+ + S_{i+1}^-) - \frac{h}{2}\sum_{i=1}^{L} c_j^\dagger c_j - c_j c_j^\dagger
\end{aligned}
$$

We find:

$$
\begin{aligned}
S_i^+ S_{i+1}^+ &= \prod_{j<i}(1-2n_j)^2 c_i^\dagger(1-2n_i)c_{i+1}^\dagger \\
S_i^- S_{i+1}^- &= \prod_{j<i}(1-2n_j)^2 c_i(1-2n_i)c_{i+1} \\
S_i^+ S_{i+1}^- &= c_i^\dagger(1-2n_i)c_{i+1} \\
S_i^- S_{i+1}^+ &= c_i(1-2n_i)c_{i+1}^\dagger
\end{aligned}
$$

Therefore:

$$
\begin{aligned}
(S_i^+ + S_i^-)(S_{i+1}^+ + S_{i+1}^-) &= (c_i^\dagger + c_i)(1-2n_i)(c_{i+1}^\dagger + c_{i+1}) \\
&= (c_i^\dagger - c_i)(c_{i+1}^\dagger + c_{i+1})
\end{aligned}
$$

Plugging in this transformation, the TFIM Hamiltonian becomes the Kitaev chain Hamiltonian:

$$
H = -\frac{J}{4}\sum_{i=1}^{L}(c_i^\dagger - c_i)(c_{i+1}^\dagger + c_{i+1}) - \frac{h}{2}\sum_{i=1}^{L} c_j^\dagger c_j - c_j c_j^\dagger
$$